Biochimica et Biophysica Acta 1863 (2017) 654–662

Contents lists available at ScienceDirect

Biochimica et Biophysica Acta

journal homepage: www.elsevier.com/locate/bbadis

A scavenger peptide prevents methylglyoxal induced pain in mice

Sebastian Brings [a,b,*], Thomas Fleming [a,c], Svenja De Buhr [b], Barbro Beijer [b], Thomas Lindner [b], Artjom Wischnjow [b], Zoltan Kender [e], Verena Peters [f], Stefan Kopf [a], Uwe Haberkorn [b], Walter Mier [b], Peter P. Nawroth [a,c,d]

[a] Department of Medicine I and Clinical Chemistry, University Hospital Heidelberg, Heidelberg, Germany
[b] Department of Nuclear Medicine, University Hospital Heidelberg, Heidelberg, Germany
[c] German Center for Diabetes Research (DZD), München-Neuherberg, Germany
[d] Joint Heidelberg-IDC Translational Diabetes Program, Helmholtz-Zentrum, München-Neuherberg, Germany
[e] Department of Medicine II, Semmelweis University, Budapest, Hungary
[f] Centre for Pediatrics and Adolescence Medicine, University Hospital Heidelberg, Heidelberg, Germany

ARTICLE INFO

Article history:
Received 26 July 2016
Received in revised form 4 November 2016
Accepted 4 December 2016
Available online 6 December 2016

Keywords:
Methylglyoxal
Scavenger
Peptide
Pain
Diabetic complications

ABSTRACT

The reactive metabolite methylglyoxal (MG) has been identified as mediator of pain. Scavenging of free MG and the prevention of MG-derived post-translational modifications may provide a useful therapeutic treatment. An arginine-rich, fatty acid coupled, cyclic peptide (CycK(Myr)R4E) with high proteolytic stability and prolonged circulation was developed for the scavenging of MG. It was shown to reduce the formation of albumin-MG adducts in vitro and prevented MG-induced pain by reducing plasma MG levels through the formation of peptide-MG adducts in vivo. CycK(Myr)R4E therefore presents a promising option for the treatment of pain and other diabetic complications associated with high MG levels.

1. Introduction

Diabetes is defined by high blood glucose levels. Despite the high efficacy of the modern standard therapies, diabetic patients develop serious complications. Diabetic complications are in part caused by reactive dicarbonyl compounds via the covalent modification of proteins resulting in advanced glycation end-products (AGEs) [1,2]. Methylglyoxal (MG) represents the most abundant reactive dicarbonyl compound in plasma of diabetic patients [3]. We have previously shown that MG is causative of hyperalgesia, an increased sensitivity towards pain, associated with diabetic neuropathy [4]. In independent studies it was shown that formation of the MG derived AGE methylglyoxal-hydroimidazolone 1 correlates with the development of diabetic nephropathy, diabetic neuropathy and diabetic retinopathy [5–7]. Thus, therapeutic lowering of MG levels is a promising approach to treat diabetic neuropathy and other diabetic complications associated with MG like diabetic nephropathy [5]. Strategies to target elevated MG levels include inducers of the MG detoxifying enzyme Glo1 and small molecule MG scavengers like aminoguanidine and alagebrium [8]. Whereas the former compounds are currently under investigation, the latter compounds failed in clinical trials due to side effects or lack of efficacy [9–11]. Alternative small molecule scavengers include creatine, arginine and pyridoxamine [12–15] but as aminoguanidine and alagebrium they suffer from a short half-life in vivo [16–19].

The scavenging reaction is a comparably slow process. Therefore the ideal scavenger has to have a long circulation time, combined with a reactivity which is specific to avoid aberrant activity [20,21]. The current first-line therapy for type 2 diabetes, metformin is a slow MG scavenger so that new scavengers must be faster than metformin. Herein, we report in vitro and in vivo data on a newly developed arginine-based MG scavenging peptide with such characteristics. This opens up new options for the treatment of pain and other diabetic complications associated with excessive MG formation.

2. Materials and methods

2.1. Animal studies

Mice were housed with a 12-hour/12-hour light/dark cycle and had free access to water and food. All procedures in this study were approved by the Animal Care and Use Committees at the Regierungspräsidium Tübingen and Karlsruhe, Germany (35-9185.81/G-3/15).

* Corresponding author at: Department of Medicine I and Clinical Chemistry, University Hospital Heidelberg, Im Neuenheimer Feld 410, 69120 Heidelberg, Germany.
E-mail address: sebastian.brings@med.uni-heidelberg.de (S. Brings).

http://dx.doi.org/10.1016/j.bbadis.2016.12.001

2.1.1. Hot plate assay and MG scavenging studies

C57BL/6 mice (Charles River, Boston, USA) were acclimatized for 1 week prior to testing. A total of 36 mice were randomly assigned to three groups. One group received the peptide CycK(Myr)R_4E (0.25 mg/mouse in 0.9% NaCl) ip while the two other groups received saline ip. One of the saline and the peptide treated group received MG (5 μg/g) iv 30 min after peptide/saline injection while the third group received saline iv. Pain response was tested using a hot plate analgesia meter (Columbus Instruments, Ohio, USA) with the plate set to 50 °C 3 h after MG injection. Mice were removed from the plate when hind pare lifting, licking, shaking or jumping occurred. Mice were removed after a maximal cut-off time of 60 s. Pain response for each animal was measured in triplicates. Plasma was collected after the hot plate assay by cardiac puncture and frozen at −80 °C.

To determine the effect of the peptide on the MG-plasma levels, mice were treated with peptide and MG as described for the pain response assay. Blood was collected through the submandibular vein into EDTA tubes 30 min after MG injection. Samples were spun for 5 min at 3000*g* at 4 °C, the supernatant frozen in liquid N_2 and stored at −80 °C until analysis. MG content was determined by LC-MS/MS analysis as described below.

2.1.2. PET analysis

DOTA coupled peptides were labeled with ^{68}Ga as described previously [22]. In short ^{68}Ga was eluted from the generator into a tube containing 20 nmol of the peptide and 0.5% ascorbic acid in 0.5 M Na-acetate buffer. The mixture was incubated at pH 3.5–4.0 for 10′ at 95 °C while stirring to allow for the ^{68}Ga-DOTA complex to form. Free ^{68}Ga was removed using C18 solid phase extraction cartridges (Thermo Scientific, USA) and the product was checked by HPLC (Agilent Technologies, USA) equipped with a radio flow detector. The labeled peptide was injected iv into NMRI mice. PET analysis was carried out for 0–1 h and for another 20 min after 2 h while cumulative images are shown for 0–20 min, 40–60 min and 120–140 min.

Data was normalized for animal weight and injected dose and pictures and data are given as standardized uptake value (SUV). For quantitative comparison the area under the curve for the SUV values of the different regions was determined and compared by Student's *t*-test.

2.2. Materials

Protected amino acids were purchased from Orpegen Peptide Chemicals (Heidelberg, Germany). All other chemicals were purchased from Sigma-Aldrich (Munich, Germany) unless indicated otherwise.

2.3. Peptide synthesis

Peptides were synthesized on solid phase, using Fmoc-chemistry. Coupling of amino acids (10 eq.) was carried out with HBTU (9.8 eq.) and DIPEA (20 eq.) in NMP and Fmoc was removed by incubation in 20% piperidine/NMP unless noted otherwise. After coupling and deprotection, resin was washed with NMP. For synthesis of CycR_4E, CycK(Myr)R_4E and CycK(DOTA)R_4E, CTC-resin (1.1 mmol/g, 200 mg) was loaded with 50 μmol Fmoc-Glu(OAll)-OH in the presence of DIPEA (2 eq.) in DCM for 1 h. Remaining active sites were capped by incubation with DCM/MeOH/DIPEA at a ratio of 17/2/1 for 30 min. Four Fmoc-Arg(Pbf)-OH were coupled and Fmoc of the fourth Fmoc-Arg(Pbf) was removed. For CycR_4E OAll was removed by incubation with Tetrakis(triphenylphosphine)palladium(0) (10 mg/100 μmol peptide) and dimethylaminoboran (50 mg/100 μmol peptide) in DCM for 20 min, next. Resin was washed with 10% ethanolamine/DCM for 5 min twice followed by washes with DCM, MeOH, DCM and NMP. CycR4E was cyclized with PyAOP (5 eq.) and DIPEA (7.5 eq.) in NMP for 1 h at RT. For CycK(Myr)R_4E and CycK(DOTA)R_4E, Alloc-Lys(Fmoc)-OH was coupled instead of palladium catalyzed removal of OAll. Next myristic acid (10 eq. with 9.8 eq. HBTU and 20 eq. DIPEA in NMP) for CycK(Myr)R_4E or DOTA-tris(tBu)ester (2 eq. with 1.8 eq. COMU and 4 eq. DIPEA in NMP overnight) for CycK(DOTA)R_4E was attached to the side chain of Lys after removal of Fmoc. CycK(Myr)R_4E and CycK(DOTA)R_4E were cyclized with diphenylphosphonic azide (7.5 eq.) and DIPEA (5 eq.) in NMP overnight after palladium catalyzed removal of Alloc and OAll as was described for CycR_4E.

The peptide standards CycK(Myr)R_3MG-H1E, CycK(Myr)R_2MG-H1E, CycK(Myr)RMG-H1R_2E and CycK(Myr)MG-H1R_3E were synthesized equivalent to CycK(Myr)R_4E while one of the four arginines was replaced with MG-H1 in each of the four arginine positions. MG-H1 was introduced as a Fmoc and bis(4-methoxyphenyl)methyl (Dod) protected amino acid (Fmoc-MG-H1(Dod)-OH) which was synthesized as described previously [23]. Coupling of Fmoc-MG-H1(Dod)-OH (2 eq.) was carried out in NMP with DIPEA (4 eq.) and COMU (1.8 eq.) for 2 h at RT and the coupling procedure was repeated once without cleaving off Fmoc.

20 pentapeptides AXRAA were synthesized, where X was replaced with one of each of the canonical amino acids. Synthesis was carried out on CTC resin (1.1 mmol/g, 100 mg resin) which was loaded with 25 μmol of Fmoc-Ala-OH in the presence of DIPEA (2 eq.) in DCM for 1 h. Subsequent amino acids were coupled and the N-terminus was acetylated by incubation with acetic anhydride (10 eq.) and DIPEA (20 eq.) for 30 min in NMP.

The peptides CycK(DOTA)K(Myr)R_4E, K(DOTA)K(Myr)R_4E and CycK(DOTA)K(Myr)MG-H1$_4$E were synthesized on Wang-Resin. MG-H1 was introduced as Fmoc-MG-H1(Dod)-OH. Resin (25 μmol) was loaded with Fmoc-Glu(OAll)-OH (2 eq.) in the presence of triphenylphosphine (3 eq.) and diisopropyl azodicarboxylate (3 eq.) in THF at RT for 2 h. Four Fmoc-Arg(Pbf)-OH or four Fmoc-MG-H1(Dod)-OH followed by Fmoc-Lys(Mtt)-OH and Alloc-Lys(Fmoc)-OH were coupled. DOTA-tris(tBu)ester and myristic acid were coupled to the side chain of Alloc-Lys(Fmoc)-OH and Fmoc-Lys(Mtt)-OH, respectively. The peptides CycK(DOTA)K(Myr)R_4E and CycK(DOTA)K(Myr)MG-H1$_4$E but not K(DOTA)K(Myr)R_4E were cyclized using diphenylphosphonic acid (7.5 eq.) and DIPEA (5 eq.) in NMP overnight after palladium catalyzed removal of Alloc and OAll as described above.

The peptides GERP$_{10}$ and K(DOTA)GERP$_{10}$ (50 μmol) were synthesized on a Rink amide resin on an ABI 433 A peptide synthesizer with 10 eq. of Fmoc-Gly-OH, Fmoc-Glu(tBu)-OH, Fmoc-Arg(Pbf)-OH, Fmoc-Pro-OH. After synthesis of GERP$_{10}$ the resin was split into two parts. One part was cleaved off of the resin and Fmoc-Lys(Alloc)-OH was added to the other part. DOTA-tris(tBu)ester was coupled after palladium catalyzed removal of Alloc as was described above.

Free peptides were obtained by incubation in TFA containing 2.5% TIS and 2.5% H_2O for 2 h at RT. Exceptions were peptides containing DOTA-tris(tBu) and MG-H1(Dod)-OH which were obtained by incubation in 5% ethandithiole in TFA for up to 24 h. Peptides were precipitated and washed in cold diethyl ether and purified by reverse phase HPLC. LC-MS analysis of peptides was carried out with an Exactive Orbitrap instrument (Thermo Scientific, USA) and results are shown in the supplement (Table S1).

2.4. Serum stability

The cyclic peptide CycK(DOTA)K(Myr)R_4E and the linear peptide K(DOTA)K(Myr)R_4E were labeled with ^{177}Lu. In short 20 nmol of peptides was incubated with ^{177}Lu in 0.4 M Na-acetate buffer (pH 5.0) for 10 min at 95 °C. Free ^{177}Lu was removed by C18 solid phase extraction cartridges, the products eluted with EtOH and checked by radio-HPLC and dried under vacuum. The radiolabelled peptides were reconstituted in human serum (H4522; Sigma-Aldrich, Germany) and incubated at 37 °C for the times indicated. Serum was precipitated by addition of two parts acetonitrile centrifuged for 10 min at 13,000*g* and the supernatant analyzed by HPLC (Agilent Technologies, USA) fitted with a radio flow detector using a 10 min gradient of 0–60% acetonitrile in water (0.1% TFA).

2.5. Inhibition of HSA MG-H1 formation

MG was synthesized as described previously [24]. In short pure MG-1,1-dimethylacetal was heated in sulphuric acid solution for 1 h and fractionally distilled in a column containing glass helices under reduced pressure. Fractions were analyzed by ^{1}H and ^{13}C NMR. The last fraction contained pure MG. Scavengers (400 μM) were incubated with HSA (400 μM) and MG (200 μM) in 0.1 M phosphate buffer pH 7.4 at 37 °C for 48 h. Two parts urea (8 M urea, 0.5 M TrisHCl; pH 8.0) were added to the solution and the sample was vortexed. HSA was precipitated by addition of two parts acetonitrile (respective to the final sample/urea mixture) and collected by centrifugation for 10 min at 13,000*g*. Peptide scavengers were not precipitated but remained in the supernatant using this procedure. The HSA containing pellet was dissolved in 20 mM HCl and the protein content was determined by BCA assay. Equal amounts of HSA were hydrolyzed by serial enzymatic digestion using pepsin, pronase E, aminopeptidase and prolidase as described previously [1]. The amount of HSA-MG-H1 adduct was determined by LC-MS. Samples and standard curve were spiked with d3-MG-H1 (Polypeptide Group, San Diego, CA, USA) and derivatized with Fmoc-Cl. Separation was performed on an Agilent 1200 Series HPLC system fitted with a C18 column (Hypersil Gold aQ; Thermo Scientific, USA) using a 20 min gradient of 0–100% acetonitrile (0.1% TFA) with the first 5 min diverted to waste. Analysis was carried out on an Exactive Orbitrap MS system (Thermo Scientific, USA). The Fmoc-MG-H1 (m + H: 451.20; m + H_{theor}:451.20) and the Fmoc-d3-MG-H1 (m + H:454.21; m + H_{theor}: 454.22) adduct eluted after 13.88 min. The calibration range used for the assay was 0–30 pmol.

2.6. MG scavenging in vitro

Scavengers (400 μM) were incubated with MG (200 μM) in 0.1 M phosphate buffer, pH 7.4 at 37 °C. The kinetics of the scavenging reaction was followed for 48 h. Samples were frozen in liquid nitrogen and stored at −80 °C until analysis. MG content was quantified by HPLC as described below.

2.7. MG quantification by HPLC and LC-MS/MS

MG was quantified using previously published methods based on HPLC for the in vitro assay or LC-MS/MS for the in vivo analysis [24]. In short samples were precipitated with 20% TCA at a ratio of 2/1 and vortex mixed. Internal standards ^{13}C MG (LC-MS/MS analysis) or 2,3-dimethylquinoxaline (HPLC analysis) and water was added and the sample mixed again. Samples were centrifuged at 13,000*g* at 4 °C for 5 min and the supernatant derivatized with 1,2-diaminobenzene in the presence of sodium azide for 4 h at RT. For HPLC based MG analysis solvent A was water + 0.1% TFA and solvent B was acetonitrile + 0.1% TFA. A linear gradient from 0 to 6% solvent B at a flow rate of 2 ml/min over 15 min was used and samples were separated on a Chromolith Performance RP18e column (3 × 100 mm, 2 μm). The MG-1,2-diaminobenzene adduct 2-methylquinoxaline and the internal standard 2,3-dimethylquinoxaline were detected with a UV monitor at 320 nm and eluted at 12.7 min and 14.2 min, respectively. For LC-MS/MS, samples were analyzed using an ACQUITY UPLC I equipped with a Xevo TQ-S mass spectrometer (Waters, USA). Samples were separated on BEH C_{18} analytical column (2.1 × 50 mm, 1.7 μm) fitted with pre-column (2.1 × 5 mm, 1.7 μm). Solvent A was water + 0.1% formic and solvent B was 50% acetonitrile + 0.1% formic acid and a linear gradient from 0 to 100% solvent B, over 10 min was used with a flow rate of 0.2 ml/min. Injection volume was 1 μl and the column temperature was 20 °C. The quinoxaline analytes were detected by electrospray positive ionization-mass spectrometric multiple-reaction monitoring (MRM). The source temperature was 150 °C and the desolvation gas temperature was 350 °C. The cone gas and desolvation gas flow rates were 150 and 800 l/h, respectively. The capillary voltage was 0.5 kV and the cone voltage was 20 V. Mass transitions (parent ion > fragment ion; collision energy) and retention times were as follows: MG 145.01 > 77.10; 24 eV, 5.93 min; [$^{13}C_3$]-MG 148.07 > 77.16; 24 eV, 5.92 min. The standard curve was in the range of 0–20 pmol and 0–1 nmol for LC MS/MS analysis and HPLC analysis, respectively.

2.8. Detection of MG-modified scavenger peptides by LC-MS/MS

Plasma was collected from mice treated with CycK(Myr)R_4E and MG as described above. In addition plasma from a type 2 diabetic was spiked with the CycK(Myr)R_4E (400 μM) immediately after collection and incubated for 24 h at 37 °C. For LC-MS/MS analysis plasma was precipitated with 2 parts acetonitrile, vortexed and centrifuged for 10 min at 13,000*g*. The supernatant was analyzed using an ACQUITY UPLC I fitted with a BEH C_{18} analytical column (2.1 × 100 mm, 1.7 μm) and pre-column (2.1 × 5 mm, 1.7 μm) and a Xevo TQ-S mass spectrometer (Waters, USA). Solvent A was water + 0.1% formic acid and solvent B was acetonitrile + 0.1% formic acid. A linear gradient from 0 to 40% solvent B at a flow rate of 0.4 ml/min over 15 min and a column temperature of 40 °C was used. Mass transitions, collision energy and retention time (parent ion > fragment ion; collision energy, retention time) were as follows:

CycK(Myr)R_4E 365.032 > 412.373; 18.0 eV and 365.032 > 335.974; 18.0 eV, 12.15 min

CycK(Myr)R_3MG-H1E 382.904 > 460.400; 16 eV and 287.543 > 312.959; 10 eV, 12.40 min

CycK(Myr)R_2MG-H1RE 382.904 > 460.400; 16 eV and 287.543 > 312.959; 10 eV, 12.50 min

CycK(Myr)RMG-H1R_2E 382.904 > 460.400; 16 eV and 287.543 > 312.959; 10 eV, 12.52 min

CycK(Myr)MG-H1R_3E 382.904 > 460.400; 16 eV and 287.543 > 312.959; 10 eV, 12.90 min.

2.9. Statistical analysis

Data was analyzed by one-way- and repeated measures ANOVA and Tukey-Kramer post-hoc test. Error bars indicate the standard error of the mean unless indicated otherwise.

3. Results

3.1. Effect of neighboring amino acid on MG scavenging activity of arginine

The main sites of MG modification of proteins are arginine residues and the AGE methylglyoxal-hydroimidazolone 1 (MG-H1) (Fig. 1 A–C) is the major resulting MG-arginine adduct. Here, we synthesized pentapeptides AcAXRAA. The second amino acid (X) was exchanged for canonical amino acids. The N-terminus of the peptides was inactivated by acetylation. Peptides (400 μM) were incubated with MG (200 μM) in 0.1 M phosphate buffer (pH 7.4) for up to 48 h and $t_{1/2}$ of MG was determined (Table 1). The fastest scavenging activity was seen in the presence of a second arginine (Ac-ARRAA), a lysine (Ac-AKRAA) and a cysteine (Ac-ACRAA) all of which bind MG whereas no strong catalytic effects of other amino acids were observed.

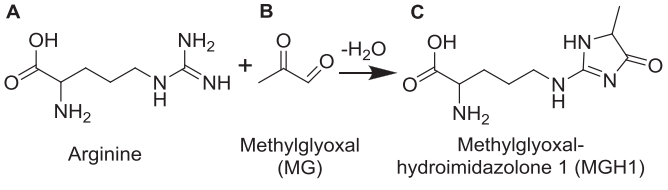

Fig. 1. Reaction of arginine (A) with MG (B) results in formation of MG-H1 (C).

Table 1
Comparison of MG scavenging kinetics of acetylated pentapeptides Ac-AXRAA. MG content was measured after co-incubation of peptide (400 μM) and MG (200 μM) at time points 0 h, 1 h, 4 h, 8 h, 24 h and 48 h in triplicates and half-life of MG was determined by non-linear regression analysis. Half-life and the 95% confidence interval of half-life are given.

Peptide	MG $t_{1/2}$ [h]	95% CI	Peptide	MG $t_{1/2}$ [h]	95% CI
Ac-ARRAA	3.69	2.89–5.13	Ac-AWRAA	9.83	8.52–11.61
Ac-AKRAA	4.02	3.33–5.08	Ac-AARAA	10.24	8.80–12.24
Ac-ACRAA	5.30	4.32–6.86	Ac-ANRAA	10.29	8.69–12.61
Ac-AGRAA	6.70	4.95–10.13	Ac-AFRAA	10.39	8.90–12.47
Ac-APRAA	7.17	5.70–9.70	Ac-AMRAA	10.56	9.47–11.93
Ac-AIRAA	8.16	6.42–11.18	Ac-ALRAA	10.76	8.62–14.32
Ac-AVRAA	9.03	6.98–12.78	Ac-AHRAA	10.95	9.25–13.41
Ac-ATRAA	9.28	7.52–12.0	Ac-ASRAA	11.06	8.52–11.61
Ac-AQRAA	9.42	8.55–15.77	Ac-ADRAA	11.62	8.10–20.56
Ac-AYRAA	9.68	8.54–11.19	Ac-AERAA	12.59	11.00–14.72

3.2. Synthesis of a myristic acid-coupled, cyclic, arginine-rich MG scavenger peptide

In previous work we reported on a 40 amino acid long MG scavenger peptide (Fig. 2 A: $GERP_{10}$) [4]. Considering the kinetics data from Table 1 a peptide with a high arginine content is best suited as MG scavenger while cyclization improves the proteolytic stability [25]. The coupling of fatty acids such as myristic acid has been shown to prolong the half-life of drugs through non-covalent interaction with albumin, previously [26,27]. Consequently, a cyclic arginine-rich peptide (Fig. 2 B: $CycR_4E$) as well as a myristic acid (Myr) coupled derivative (Fig. 2 C and D: $CycK(Myr)R_4E$) were synthesized to test their scavenging activity. A cyclization strategy via the glutamic acid side chain was chosen due to greater flexibility with regard to the conjugation of variable groups to the lysine side chain.

3.3. Scavenging activity in vitro and comparison with small molecule scavengers

The effect of the scavenger peptides was first tested in vitro. Albumin is the most abundant plasma protein and contains 24 arginine residues 21 of which are capable of participating in the glycation reaction leading to irreversible protein modifications [28]. We determined whether MG scavengers are capable of preventing the formation of albumin-MG-H1 modifications. The activity of the scavenger peptides was tested in parallel to several small molecules (Fig. 3 A), previously described to bind MG or other reactive carbonyls. Amongst the latter were the endogenous molecules carnosine (Car), creatine (Cre) and the vitamer pyridoxamine (Pyr), the investigational drugs aminoguanidine (Agd) and alagebrium (Ala) and the widely prescribed anti-diabetic drug metformin (Met) [13,15,20,29–31]. As the scavenger peptide consists of arginine residues, acetylated arginine (AcR) was also tested. The scavengers (400 μM) were incubated with MG (200 μM) in the presence of human serum albumin (HSA, 400 μM) at 37 °C for 48 h in 0.1 M phosphate buffer (pH 7.4). $CycK(Myr)R_4E$ was also tested at 100 μM ($CycK(Myr)R_4E$ to correct for the higher number of active sites. HSA was subsequently analyzed for MG-H1 content (Fig. 3 B and C). The kinetics of MG scavenging were determined in parallel (Table 2). Scavengers (400 μM) were incubated with MG (200 μM) in 0.1 M phosphate buffer at 37 °C and $t_{1/2}$ of MG was determined. The scavenger peptides, $CycK(Myr)R_4E$, $CycR_4E$ and $GERP_{10}$ were similar to alagebrium in terms of the prevention of HSA-MG-H1 formation (Fig. 3 B). $CycK(Myr)R_4E$ when added at 1/4th the molar concentration (100 μM) of the small molecular scavengers was equally fast at scavenging MG as AcR which features the same active site (Table 2). However, $CycK(Myr)R_4E$ at 100 μM but not AcR at 400 μM significantly prevented HSA-MG-H1 formation (Fig. 3 B and C). This could be due to non-covalent interactions of AcR with albumin possibly resulting in a decreased activity [32]. Such interactions are likely to be weaker in a larger molecule like $CycK(Myr)R_4E$ due to steric hindrance. MG scavenging activity was also measured for a co-incubation of Met with $CycK(Myr)R_4E$ (400 μM and 100 μM labeled low) to determine whether the peptide has an effect in addition to Met (Table 2). The co-incubations showed a similar activity as the incubations of $CycK(Myr)R_4E$ alone confirming an additive effect of $CycK(Myr)R_4E$ to Met. Agd scavenged MG faster and was more efficient at preventing HSA-MG-H1 adduct formation than the scavenger peptides but clinical trials of this compound failed due to side effects [9]. Metformin and pyridoxamine were slow MG scavengers which did

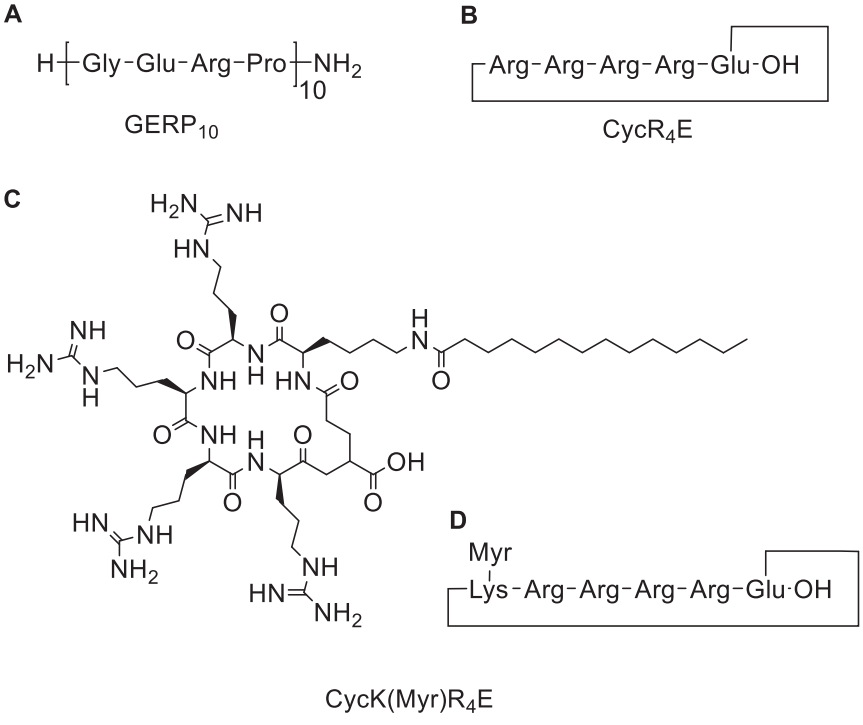

Fig. 2. Schematic drawings of the scavenger peptides $GERP_{10}$ (A), $CycR_4E$ (B) and structure (C) and schematic drawing (D) for $CycK(Myr)R_4E$.

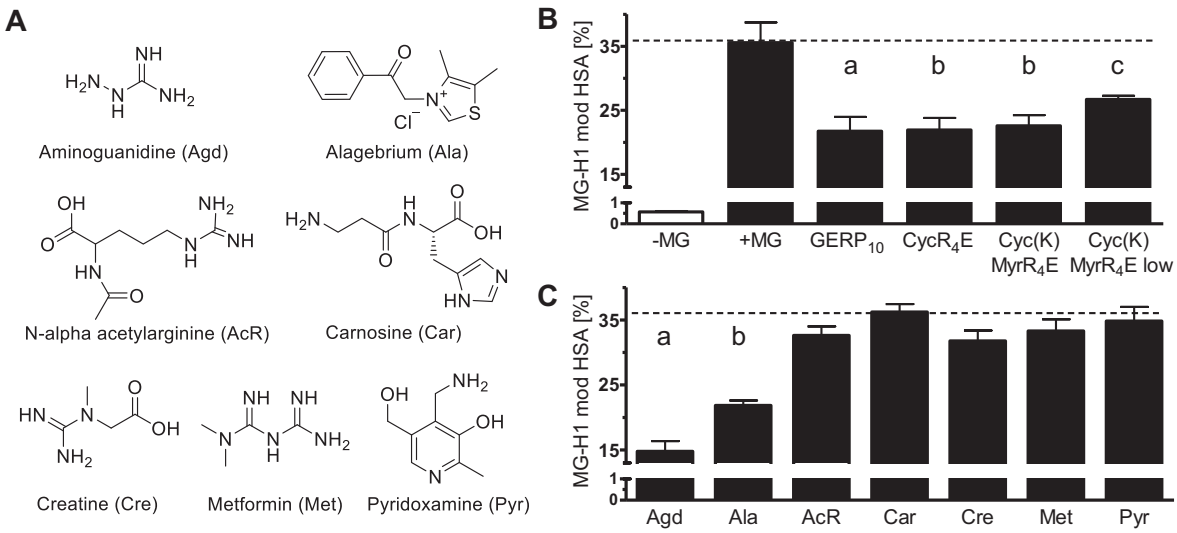

Fig. 3. Structures of small molecule MG scavengers (A). Competitive scavenging activity of peptides (B) and small molecules (C) in the presence of HSA. HSA (400 μM) was incubated without MG (−MG), with 200 μM MG (+MG) or with 200 μM MG and the indicated scavenger molecules (400 μM) for 24 h and MG-H1 modified albumin was quantified. The dashed line indicates the level of MG modified HSA (+MG) in the absence of scavengers. CycK(Myr)R_4E scavenging activity was also tested at 100 μM (CycK(Myr)R_4E low). Data was analyzed by one-way ANOVA and Tukey-Kramer post-hoc test; a: $p < 0.001$, b: $p < 0.01$ and c: $p < 0.05$ vs. +MG.

not significantly prevent HSA-MG-H1 formation. Creatine was the fastest of the endogenous MG scavengers tested but only a trend for the prevention of HSA-MG-H1 formation in vitro was observed. The dipeptide carnosine neither scavenged MG nor did it prevent HSA-MG-H1 formation. This is in contrast to the scavenging effect of carnosine on the reactive aldehyde 4-hydroxytrans-2-nonenal [31].

3.4. Stability, biodistribution and pharmacokinetics of scavenger peptides

A long circulatory time is mandatory for the scavenger peptide to bind MG and it must therefore be stable towards proteolysis. The cyclic peptide and a linear control peptide were modified with the chelator DOTA (CycK(DOTA)K(Myr)R_4E, see structure in Fig. S1 A; K(DOTA)K(Myr)R_4E, see structure in Fig. S1 B). Modified peptides were labeled with ^{177}Lu, incubated with HSA at 37 °C and analyzed by HPLC equipped with a radio flow detector at indicated times. Cyclic CycK(DOTA)K(Myr)R_4E is much more stable than the linear counterpart K(DOTA)K(Myr)R_4E with 86.16% vs. 33.4% of the peptide remaining after 24 h, respectively (Fig. 4 A).

Using PET, the biodistribution and pharmacokinetics of the cyclic, myristic acid coupled CycK(DOTA)K(Myr)R_4E peptide was compared to fatty acid free K(DOTA)$GERP_{10}$ and CycK(DOTA)R_4E in mice. In brief, DOTA derivatives (see Fig. S1 A, C and D) of the peptides were labeled with ^{68}Ga, administered iv to mice and distribution followed by PET for t_1 = 0–20 min, t_2 = 20–40 min, t_3 = 40–60 min and t_4 = 120–140 min and SUV values for kidneys, bladder, liver, heart and muscle were calculated. Fatty acid free K(DOTA)$GERP_{10}$ as well as CycK(DOTA)R_4E were excreted almost completely within 20 min while the myristic acid coupled peptide CycK(DOTA)K(Myr)R_4E circulated for over 2 h most likely due to its interaction with albumin (SUV for kidneys and bladder in Fig. 4 B and heart, muscle and liver in Fig. 4 C). Representative PET images after 0–20 min and 120–140 min are shown for K(DOTA)$GERP_{10}$ (Fig. 4 D), CycK(DOTA)R_4E (Fig. 4 E) and CycK(DOTA)K(Myr)R_4E (Fig. 4 F).

Table 2
MG scavenging kinetics of MG scavenger peptides and small molecule carbonyl scavengers. MG content was measured after co-incubation of scavenger (400 μM) and MG (200 μM) at time points 0 h, 1 h, 4 h, 8 h, 24 h and 48 h in triplicates and half-life of MG was determined by non-linear regression analysis. CycK(Myr)R_4E kinetics were also measured at 100 μM labeled low and co-incubated in the presence of Met. Half-life and the 95% confidence interval of the half-life are given.

Scavenger	MG $t_{1/2}$ [h]	95% CI
Agd	0.24	0.15–0.58
Ala	0.77	0.68–0.88
$GERP_{10}$	1.36	1.13–1.70
CycR_4E	1.95	1.66–2.37
CycK(Myr)R_4E	3.28	2.80–3.96
Met + CycK(Myr)R_4E	3.84	3.64–4.06
AcR	6.66	5.67–8.08
CycK(Myr)R_4E low	6.72	4.66–12.01
Met + CycK(Myr)R_4E low	6.92	5.85–8.47
Cre	7.36	6.24–8.96
Met	17.29	14.54–21.33
Pyr	20.90	18.65–23.77
Car	138.1	103.50–207.60

3.5. Scavenging activity in vivo

Based upon the pharmacokinetics and scavenging results the peptide CycK(Myr)R_4E was chosen for testing of MG scavenging activity in mice. Mice were injected with the peptide ip (0.25 mg/mouse) 30 min prior to injection with MG iv (5 μg/g body weight). Plasma was collected via the mandibular vein 30 min after MG injection and analyzed for MG levels by LC-MS/MS. Control mice had MG plasma levels of approximately 150 nmol/l whereas MG injection resulted in increased MG plasma levels which was lowered by treatment with CycK(Myr)R_4E (Fig. 5 A).

Elevated MG plasma levels are associated with hyperalgesia, an increased sensitivity towards pain, in diabetic patients while injection of MG produces hyperalgesia in mice via modification of proteins [4,33]. To assess whether decreased MG levels upon peptide treatment were associated with an improvement of hyperalgesia, mice were treated as described for the determination of MG plasma levels. The effect of the peptide on MG induced hyperalgesia was assessed by hot-plate assay 3 h after MG injection. Values were normalized for the average response time of the control animals (20.75 s ± 0.60 s). Mice which received MG displayed hyperalgesia while treatment with the MG-scavenging peptide CycK(Myr)R_4E prior to MG injection resulted in an almost complete normalization of hyperalgesia (Fig. 5 B).

MG-H1 represents the most frequently formed arginine-MG adduct. Modification of CycK(Myr)R_4E with MG is therefore likely to result in an MG-H1 modified peptide. To establish whether this was the case, the plasma from the mice treated with the peptide and MG was analyzed

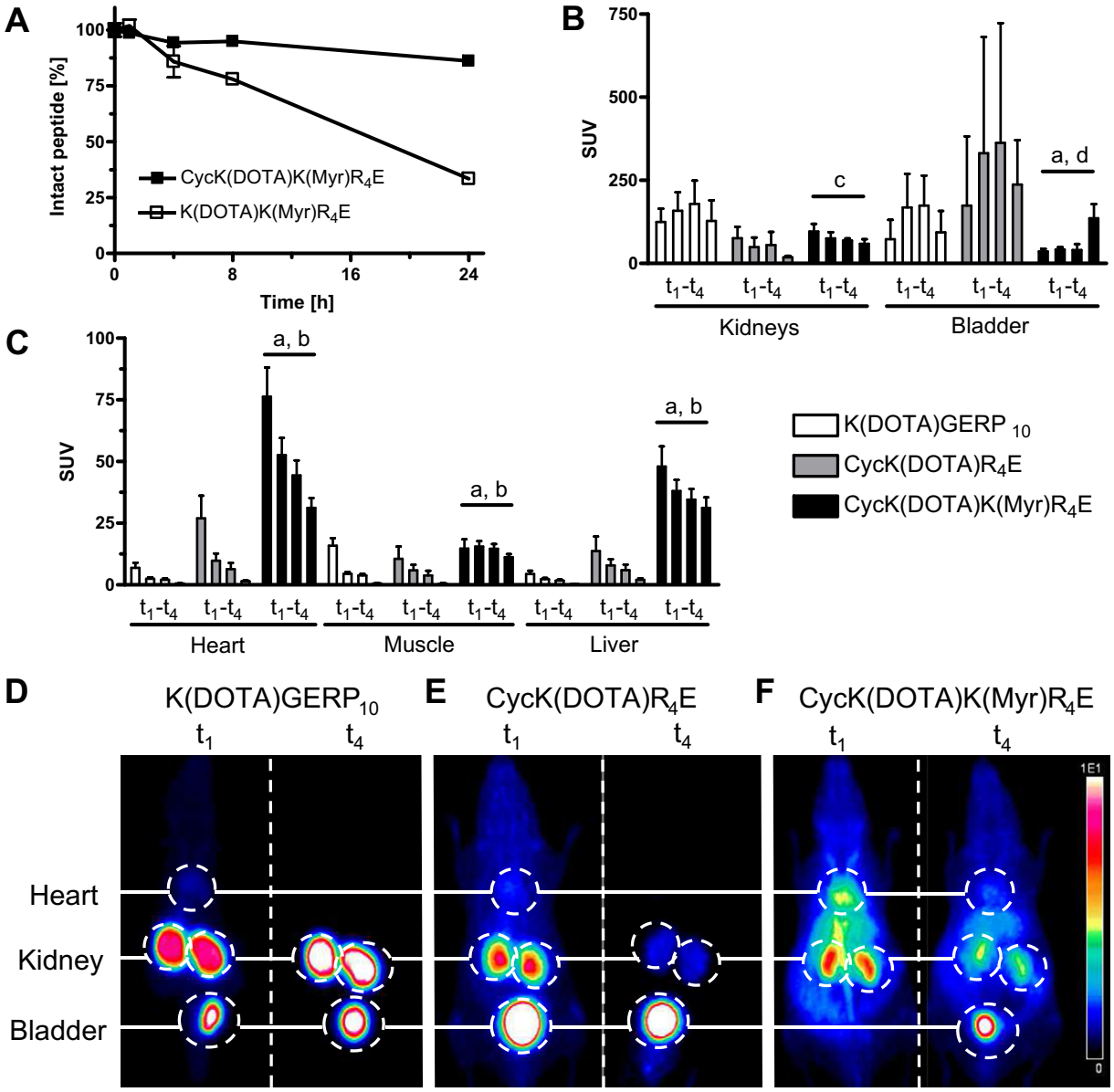

Fig. 4. Serum stability analysis (A) of fatty acid coupled linear (K(DOTA)K(Myr)R_4E) vs. cyclic peptide (CycK(DOTA)K(Myr)R_4E). Peptides were labeled with ^{177}Lu, incubated in serum at 37 °C and analyzed at indicated times by radio HPLC. PET analysis of ^{68}Ga-labeled scavenger peptides K(DOTA)$GERP_{10}$, CycK(DOTA) R_4E and CycK(DOTA)K(Myr)R_4E was carried out in NMRI-mice. SUV values for the kidney and bladder (B) as well as heart, muscle and liver (C) for K(DOTA)$GERP_{10}$ white bars), CycK(DOTA)R_4E (grey bars) and CycK(DOTA)K(Myr)R_4E (black bars) were quantitated. Indicated time points are t_1 = 0–20 min, t_2 = 20–40 min, t_3 = 40–60 min and t_4 = 120–140 min. Representative PET images are shown for t_1 and t_4 for K(DOTA)$GERP_{10}$(D), CycK(DOTA)R_4E (E) and CycK(DOTA)K(Myr)R_4E (F). Data was analyzed by repeated measures ANOVA and Tukey-Kramer post-hoc test; a: $p < 0.001$ vs. CycK(DOTA)R_4E; b: $p < 0.001$ vs. K(DOTA)$GERP_{10}$; c: $p < 0.01$ vs. K(DOTA)$GERP_{10;}$ d: $p < 0.05$ vs. K(DOTA)$GERP_{10}$ of respective organs.

for the presence of the MG-H1 modified peptide. To achieve this, four peptides with one MG-H1 replacing each of the four arginine positions (see Fig. S1 E–H: MG-adduct # 1–4) were synthesized as standards using Fmoc-MG-H1(Dod)-OH [23]. The respective MG-H1 modified peptides were subsequently detected by LC-MS/MS. MG-H1 modified peptides (MG-adducts # 1–3) were detectable in mice which received the peptide prior to MG injection (Fig. 5 C) showing that the peptide scavenges MG in vivo. Scavenging effect of the peptide was also tested in plasma donated from a patient with type 2 diabetes where MG-adducts # 1–4 were observed (Fig. 5 D).

3.6. Biodistribution and pharmacokinetics of MG-H1 modified peptide

It was previously shown that AGE modification of proteins triggers their uptake by the kidneys and the liver [34]. The resulting increased proteolytic load may contribute to the development of diabetic complications and other age related diseases [35,36]. A DOTA conjugated derivative of a MG-H1 modified scavenger peptide (CycK(DOTA)K(Myr)MG-H1$_4$E, see structure in Fig. S1 I) was synthesized to determine whether a potentially pathogenic elevated uptake of the MG-H1 modified peptide into the kidney and liver can be observed. The MG-H1 modified scavenger peptide was compared to the unmodified scavenger peptide (CycK(DOTA)K(Myr)R_4E; structure in Fig. S1 A) by PET. Peptides were again labeled with ^{68}Ga, administered iv to mice and distribution was followed by PET for t_1 = 0–20 min, t_2 = 20–40 min, t_3 = 40–60 min and t_4 = 120–140 min. SUV values for kidneys, bladder, liver, heart and muscle were calculated.

The level of the MG-H1 modified peptide was higher in the bladder (Fig. 6A) while levels in the kidneys were lower with a trend for lower levels in the liver. The levels in the muscle and heart (Fig. 6 B) were

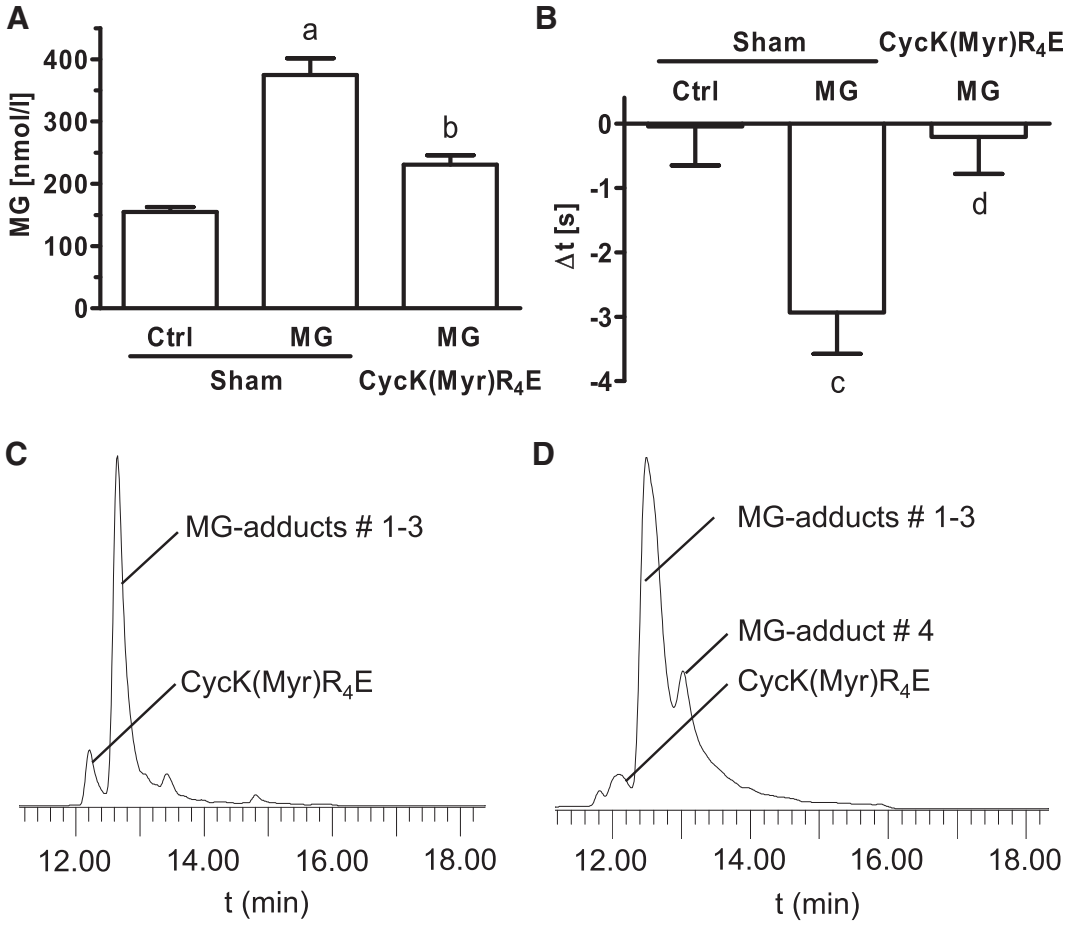

Fig. 5. Efficacy of the MG scavenger CycK(Myr)R_4E in mice. Mice were injected with CycK(Myr)R_4E or saline solution (Sham) 30 min prior to MG injection or saline injection (Ctrl). MG plasma levels were determined 30 min after MG injection (A). The effect of the peptide on pain sensitivity was determined by hot-plate assay 3 h after MG injection (B). The MG-peptide adducts were detected in plasma of mice 3 h after MG injection (C) as well as in plasma from a diabetic patient spiked with the peptide (D). Data was analyzed by one-way ANOVA and Tukey-Kramer post-hoc test; a: $p < 0.001$ vs. Ctrl/Sham; b: $p < 0.001$ vs. MG/Sham; c: $p < 0.01$ vs. Ctrl/Sham; d: $p < 0.01$ vs. MG/Sham.

similar for both peptides. Representative PET images are presented for the unmodified peptide (Fig. 6 C) and modified peptide (Fig. 6 D). Thus the modified peptide was readily excreted via the kidneys and the bladder without a potentially pathogenic accumulation in the excretory organs.

4. Conclusion

Diabetic complications are in part caused by methylglyoxal while therapeutic lowering of MG has been unsuccessful to date. Clinical trials of the small molecule MG scavengers aminoguanidine and alagebrium have been terminated due to side effects or lack of efficacy [9]. Alternative small molecule scavengers like creatine, free arginine and pyridoxamine are being investigated but suffer from a short half-life [12–14,16–19].

Interestingly metformin the current first-line therapy for the treatment of type 2 diabetes is a slow MG scavenger [37]. Even the slow MG scavenging kinetics of metformin could provide a therapeutic effect. In support of this, metformin reduces systemic MG levels and recently a MG-metformin adduct was detected in urine at concentrations up to 4 μM [15,38,39]. Consequently, an improved MG scavenger must bind MG faster than metformin to yield additional benefits to patients already treated with this drug.

Here, we developed such a peptide which scavenges MG faster than metformin and has a long circulation time. In summary, CycK(Myr)R_4E, efficiently scavenges MG and prevents the formation of HSA-MG-H1 adducts in vitro. The peptide significantly reduces MG plasma levels and normalizes MG-induced hyperalgesia in mice. Cyclization contributes to the increased plasma stability while the attachment of myristic acid improves peptide half-life most likely through non-covalent binding of albumin. PET analysis revealed that the MG-modified peptide is excreted via the kidneys, without accumulation in the latter. The pharmacokinetic and pharmacodynamic properties of CycK(Myr)R_4E therefore make it a promising candidate for the treatment of diabetic neuropathy and other diabetic complications which are associated with increased plasma levels of the reactive metabolite MG.

Author contributions

Sebastian Brings designed and carried out the experiments, analyzed and interpreted the data and wrote the manuscript. Thomas Fleming designed and carried out experiments, analyzed the data and revised the manuscript. Svenja de Buhr carried out experiments. Barbro Beijer synthesized precursors. Thomas Lindner synthesized precursors. Artjom Wischnjow synthesized peptides and revised the manuscript. Zoltan Kender revised the manuscript. Verena Peters revised the manuscript. Stefan Kopf contributed patient samples. Uwe Haberkorn revised the manuscript and planned the molecular imaging issues. Walter Mier designed and supervised experiments, interpreted the data and revised the manuscript. Peter P. Nawroth designed and supervised the experiments interpreted the data and revised the manuscript.

Funding

This work was supported by the Deutsche Forschungsgemeinschaft (DFG; SFB1118), the Dietmar Hopp Foundation (DHS) and the German

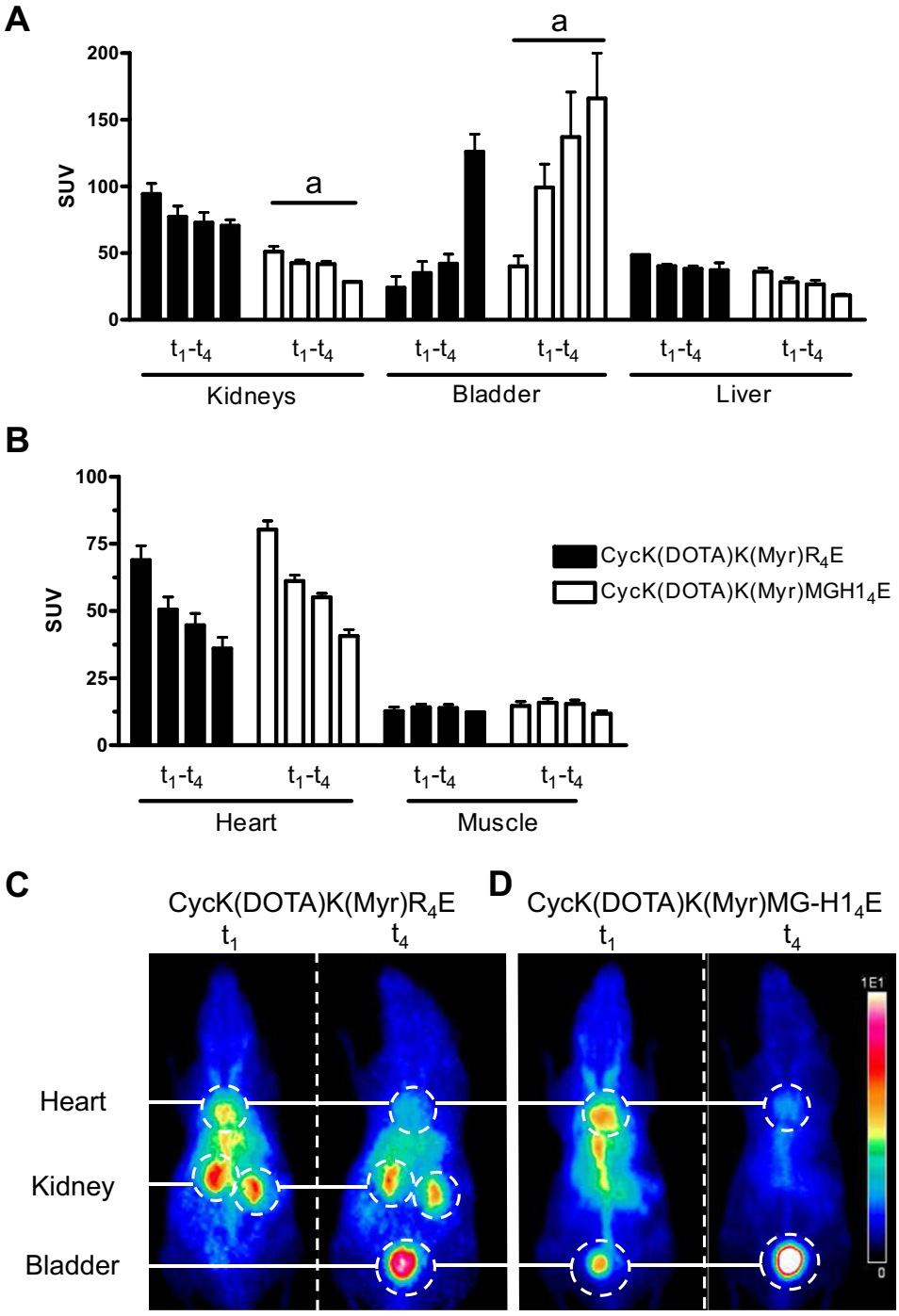

Fig. 6. Biodistribution of unmodified vs. MG modified scavenger peptide. Mice were injected with CycK(DOTA)K(Myr)R_4E (black bars) or its MG modified derivative CycK(DOTA)K(Myr)MG-$H1_4$E (white bars) and analyzed by PET. Standardized uptake values (SUV) for kidneys, bladder and liver (A) as well as heart and muscle (B) are given with $n = 3$ per peptide. Indicated time points are t_1 = 0–20 min, t_2 = 20–40 min, t_3 = 40–60 min and t_4 = 120–140 min. Representative PET images are shown for t_1 and t_3 for CycK(DOTA)K(Myr)R_4E (C) and CycK(DOTA)K(Myr)MGH1_4E (D). Data was analyzed by repeated measures ANOVA and Tukey-Kramer post-hoc test; a: $p < 0.001$ vs. CycK(DOTA)K(Myr)R_4E of respective organ.

Center for Diabetes Research (DZD; FKZ: 82DZD00702) and the Interdisciplinary Neurobehavioural Core facility of the University of Heidelberg (INBC).

Conflict of interest statement

Sebastian Brings, Thomas Fleming, Walter Mier and Peter P. Nawroth are named as inventors in a pending patent that discloses the use of scavenger peptides for the treatment of MG induced complications.

Transparency document

The Transparency document associated with this article can be found, in online version.

Acknowledgements

We would like to thank the Interdisciplinary Neurobehavioral Core for support with the pain sensitivity tests and Karin Leotta for PET analysis. We thank Axel Erhardt for excellent technical assistance.

Appendix A. Supplementary data

Supplementary data to this article can be found online at http://dx.doi.org/10.1016/j.bbadis.2016.12.001.

References

[1] P.J. Thornalley, S. Battah, N. Ahmed, N. Karachalias, S. Agalou, R. Babaei-Jadidi, A. Dawnay, Quantitative screening of advanced glycation endproducts in cellular and extracellular proteins by tandem mass spectrometry, Biochem. J. 375 (2003) 581–592.

[2] N. Rabbani, P.J. Thornalley, The critical role of methylglyoxal and glyoxalase 1 in diabetic nephropathy, Diabetes 63 (2014) 50–52.

[3] T. Fleming, J. Cuny, G. Nawroth, Z. Djuric, P.M. Humpert, M. Zeier, A. Bierhaus, P.P. Nawroth, Is diabetes an acquired disorder of reactive glucose metabolites and their intermediates? Diabetologia 55 (2012) 1151–1155.

[4] A. Bierhaus, T. Fleming, S. Stoyanov, A. Leffler, A. Babes, C. Neacsu, S.K. Sauer, M. Eberhardt, M. Schnolzer, F. Lasitschka, W.L. Neuhuber, T.I. Kichko, I. Konrade, R. Elvert, W. Mier, V. Pirags, I.K. Lukic, M. Morcos, T. Dehmer, N. Rabbani, P.J. Thornalley, D. Edelstein, C. Nau, J. Forbes, P.M. Humpert, M. Schwaninger, D. Ziegler, D.M. Stern, M.E. Cooper, U. Haberkorn, M. Brownlee, P.W. Reeh, P.P. Nawroth, Methylglyoxal modification of Nav1.8 facilitates nociceptive neuron firing and causes hyperalgesia in diabetic neuropathy, Nat. Med. 18 (2012) 926–933.

[5] P.J. Beisswenger, K.S. Drummond, R.G. Nelson, S.K. Howell, B.S. Szwergold, M. Mauer, Susceptibility to diabetic nephropathy is related to dicarbonyl and oxidative stress, Diabetes 54 (2005) 3274–3281.

[6] P.J. Beisswenger, S.K. Howell, G.B. Russell, M.E. Miller, S.S. Rich, M. Mauer, Early progression of diabetic nephropathy correlates with methylglyoxal-derived advanced glycation end products, Diabetes Care 36 (2013) 3234–3239.

[7] S. Genuth, W. Sun, P. Cleary, X. Gao, D.R. Sell, J. Lachin, D.E.R. Group, V.M. Monnier, Skin advanced glycation end products glucosepane and methylglyoxal hydroimidazolone are independently associated with long-term microvascular complication progression of type 1 diabetes, Diabetes 64 (2015) 266–278.

[8] M. Xue, M.O. Weickert, S. Qureshi, N.B. Kandala, A. Anwar, M. Waldron, A. Shafie, D. Messenger, M. Fowler, G. Jenkins, N. Rabbani, P.J. Thornalley, Improved glycemic control and vascular function in overweight and obese subjects by glyoxalase 1 inducer formulation, Diabetes 65 (2016) 2282–2294.

[9] J.M. Forbes, M.E. Cooper, Mechanisms of diabetic complications, Physiol. Rev. 93 (2013) 137–188.

[10] D.E. Maessen, C.D. Stehouwer, C.G. Schalkwijk, The role of methylglyoxal and the glyoxalase system in diabetes and other age-related diseases, Clin. Sci. (Lond.) 128 (2015) 839–861.

[11] L. Engelen, C.D. Stehouwer, C.G. Schalkwijk, Current therapeutic interventions in the glycation pathway: evidence from clinical studies, Diab. Obes. Metab. 15 (2013) 677–689.

[12] I. Dhar, A. Dhar, L. Wu, K. Desai, Arginine attenuates methylglyoxal- and high glucose-induced endothelial dysfunction and oxidative stress by an endothelial nitric-oxide synthase-independent mechanism, J. Pharmacol. Exp. Ther. 342 (2012) 196–204.

[13] J. Lobner, J. Degen, T. Henle, Creatine is a scavenger for methylglyoxal under physiological conditions via formation of *N*-(4-methyl-5-oxo-1-imidazolin-2-yl)sarcosine (MG-HCr), J. Agric. Food Chem. 63 (2015) 2249–2256.

[14] P.A. Voziyan, T.O. Metz, J.W. Baynes, B.G. Hudson, A post-Amadori inhibitor pyridoxamine also inhibits chemical modification of proteins by scavenging carbonyl intermediates of carbohydrate and lipid degradation, J. Biol. Chem. 277 (2002) 3397–3403.

[15] O.R. Kinsky, T.L. Hargraves, T. Anumol, N.E. Jacobsen, J. Dai, S.A. Snyder, T.J. Monks, S.S. Lau, Metformin scavenges methylglyoxal to form a novel imidazolinone metabolite in humans, Chem. Res. Toxicol. 29 (2016) 227–234.

[16] S.M. Bode-Boger, R.H. Boger, A. Galland, D. Tsikas, J.C. Frolich, L-Arginine-induced vasodilation in healthy humans: pharmacokinetic-pharmacodynamic relationship, Br. J. Clin. Pharmacol. 46 (1998) 489–497.

[17] A.M. Persky, G.A. Brazeau, Clinical pharmacology of the dietary supplement creatine monohydrate, Pharmacol. Rev. 53 (2001) 161–176.

[18] T. Sakurai, T. Asakura, A. Mizuno, M. Matsuda, Absorption and metabolism of pyridoxamine in mice. I. Pyridoxal as the only form of transport in blood, J. Nutr. Sci. Vitaminol. (Tokyo) 37 (1991) 341–348.

[19] T. Sakurai, T. Asakura, A. Mizuno, M. Matsuda, Absorption and metabolism of pyridoxamine in mice. II. Transformation of pyridoxamine to pyridoxal in intestinal tissues, J. Nutr. Sci. Vitaminol. (Tokyo) 38 (1992) 227–233.

[20] T.W. Lo, T. Selwood, P.J. Thornalley, The reaction of methylglyoxal with aminoguanidine under physiological conditions and prevention of methylglyoxal binding to plasma proteins, Biochem. Pharmacol. 48 (1994) 1865–1870.

[21] D.J. Borg, J.M. Forbes, Targeting advanced glycation with pharmaceutical agents: where are we now? Glycoconj. J. 33 (2016) 653–670.

[22] A. Wischnjow, D. Sarko, M. Janzer, C. Kaufman, B. Beijer, S. Brings, U. Haberkorn, G. Larbig, A. Kubelbeck, W. Mier, Renal targeting: peptide-based drug delivery to proximal tubule cells, Bioconjug. Chem. (2016).

[23] T. Wang, R. Kartika, D.A. Spiegel, Exploring post-translational arginine modification using chemically synthesized methylglyoxal hydroimidazolones, J. Am. Chem. Soc. 134 (2012) 8958–8967.

[24] N. Rabbani, P.J. Thornalley, Measurement of methylglyoxal by stable isotopic dilution analysis LC-MS/MS with corroborative prediction in physiological samples, Nat. Protoc. 9 (2014) 1969–1979.

[25] P. Li, P.P. Roller, Cyclization strategies in peptide derived drug design, Curr. Top. Med. Chem. 2 (2002) 325–341.

[26] I. Jonassen, S. Havelund, T. Hoeg-Jensen, D.B. Steensgaard, P.O. Wahlund, U. Ribel, Design of the novel protraction mechanism of insulin degludec, an ultra-long-acting basal insulin, Pharm. Res. 29 (2012) 2104–2114.

[27] R.E. Kontermann, Strategies for extended serum half-life of protein therapeutics, Curr. Opin. Biotechnol. 22 (2011) 868–876.

[28] J. Anguizola, R. Matsuda, O.S. Barnaby, K.S. Hoy, C. Wa, E. DeBolt, M. Koke, D.S. Hage, Review: glycation of human serum albumin, Clin. Chim. Acta 425 (2013) 64–76.

[29] A. Dhar, K.M. Desai, L. Wu, Alagebrium attenuates acute methylglyoxal-induced glucose intolerance in Sprague-Dawley rats, Br. J. Pharmacol. 159 (2010) 166–175.

[30] R.H. Nagaraj, P. Sarkar, A. Mally, K.M. Biemel, M.O. Lederer, P.S. Padayatti, Effect of pyridoxamine on chemical modification of proteins by carbonyls in diabetic rats: characterization of a major product from the reaction of pyridoxamine and methylglyoxal, Arch. Biochem. Biophys. 402 (2002) 110–119.

[31] G. Vistoli, M. Orioli, A. Pedretti, L. Regazzoni, R. Canevotti, G. Negrisoli, M. Carini, G. Aldini, Design, synthesis, and evaluation of carnosine derivatives as selective and efficient sequestering agents of cytotoxic reactive carbonyl species, Chem. Med. Chem. 4 (2009) 967–975.

[32] D. Shah, A.R. Shaikh, X. Peng, R. Rajagopalan, Effects of arginine on heat-induced aggregation of concentrated protein solutions, Biotechnol. Prog. 27 (2011) 513–520.

[33] M.J. Eberhardt, M.R. Filipovic, A. Leffler, J. de la Roche, K. Kistner, M.J. Fischer, T. Fleming, K. Zimmermann, I. Ivanovic-Burmazovic, P.P. Nawroth, A. Bierhaus, P.W. Reeh, S.K. Sauer, Methylglyoxal activates nociceptors through transient receptor potential channel A1 (TRPA1): a possible mechanism of metabolic neuropathies, J. Biol. Chem. 287 (2012) 28291–28306.

[34] R. Nagai, K. Mera, K. Nakajou, Y. Fujiwara, Y. Iwao, H. Imai, T. Murata, M. Otagiri, The ligand activity of AGE-proteins to scavenger receptors is dependent on their rate of modification by AGEs, Biochim. Biophys. Acta 1772 (2007) 1192–1198.

[35] S. Brings, S. Zhang, Y.S. Choong, S. Hogl, M. Middleditch, M. Kamalov, M.A. Brimble, D. Gong, G.J. Cooper, Diabetes-induced alterations in tissue collagen and carboxymethyllysine in rat kidneys: association with increased collagen-degrading proteinases and amelioration by Cu(II)-selective chelation, Biochim. Biophys. Acta 1852 (2015) 1610–1618.

[36] T. Uchiki, K.A. Weikel, W. Jiao, F. Shang, A. Caceres, D. Pawlak, J.T. Handa, M. Brownlee, R. Nagaraj, A. Taylor, Glycation-altered proteolysis as a pathobiologic mechanism that links dietary glycemic index, aging, and age-related disease (in nondiabetics), Aging Cell 11 (2012) 1–13.

[37] S.E. Inzucchi, R.M. Bergenstal, J.B. Buse, M. Diamant, E. Ferrannini, M. Nauck, A.L. Peters, A. Tsapas, R. Wender, D.R. Matthews, A. American Diabetes, D. European Association for the Study of, Management of hyperglycemia in type 2 diabetes: a patient-centered approach: position statement of the American Diabetes Association (ADA) and the European Association for the Study of Diabetes (EASD), Diabetes Care 35 (2012) 1364–1379.

[38] P.J. Beisswenger, S.K. Howell, A.D. Touchette, S. Lal, B.S. Szwergold, Metformin reduces systemic methylglyoxal levels in type 2 diabetes, Diabetes 48 (1999) 198–202.

[39] P. Beisswenger, D. Ruggiero-Lopez, Metformin inhibition of glycation processes, Diabete Metab. 29 (2003), 6S95–103. .